

## Supporting Information

November 22, 2013

### **Tuneable Multicoloured Patterns From Photonic Cross Communication Between Cholesteric Liquid Crystal Droplets**

*JungHyun Noh, Hsin-Ling Liang, Irena Drevensek-Olenik and Jan P. F. Lagerwall*

#### **1 Confirming the radial helix orientation**

The radial helix configuration in cholesteric droplets produced in the N\* phase is easily verified from their optical properties in reflection, as shown in Fig. 1. (If the liquid crystal is heated to the isotropic state during droplet production the alignment is much less uniform with consequently less well defined optical characteristics.) When viewed along the helix a distinct colour from selective reflection is seen, the same as when a flat sample of the same liquid crystal is observed (see Fig. 2 for a concise explanation of the optical properties of cholesterics). In a droplet with radial helix orientation this viewing direction occurs only at the droplet centre, hence this is where we see a coloured spot in each droplet. Fig. 1 shows hexagonally close-packed colloidal crystal structures formed by droplets of three different liquid crystal mixtures, their compositions being tuned for blue (a), green (b) and red (c) selective reflection, respectively. In the inset of Fig. 1(b) a single green-reflecting droplet is viewed through a circular analyser, set for right- and left-handed polarisation, respectively. The disappearance of the central spot in the second case demonstrates that the reflected light is right-handed, hence also the helix is right-handed.

In panel (c) there are two additional superposed hexagonal patterns, shifted 30° with respect to each other, each one with a blue-green spot near the periphery and a green-yellow spot slightly closer to the centre. (Their origin is explained in the main text.) The spots are quite blurred in some droplets and frequently parts of the pattern are missing. Moreover, the colours of the reflection spots are slightly false because these droplets were collected in a plastic petri dish and the birefringence of the plastic gives a contribution to the polarising microscopy image that turns the background coloured rather than black and it distorts the colour of all selective reflection phenomena.

The larger the droplet size the easier and more accurate the characterization, hence the droplets in Fig. 2 and in the main paper are quite large, several hundred  $\mu\text{m}$  in

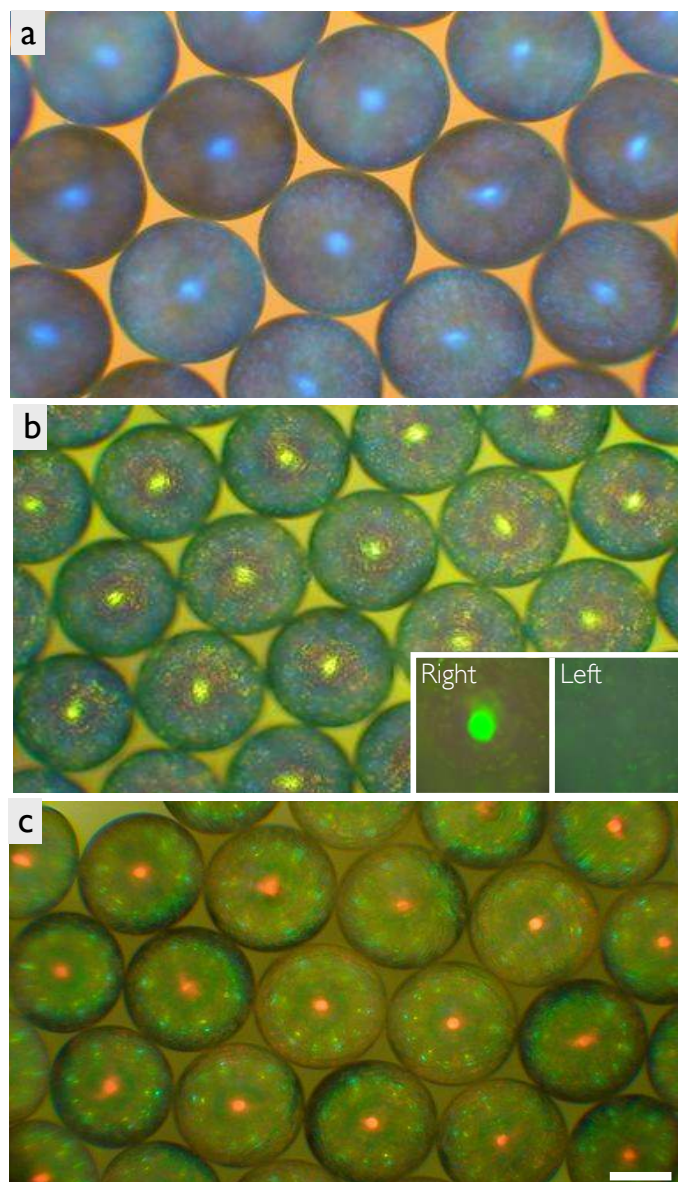


Figure 1: Hexagonal close-packed colloidal crystals of droplets of cholesteric liquid crystal mixtures giving normal-incidence selective reflection in the blue (a), green (b) and red (c), respectively. The background colour between the droplets is due to the birefringence of the plastic petri dish used for collecting the droplets. As a consequence of the right-handed cholesteric helix the reflected light is right-handed circular polarised, as confirmed in the inset of (b), where a green-reflecting droplet is observed through right- and left-handed circular analysers, respectively. Scale bar is 200  $\mu\text{m}$ .

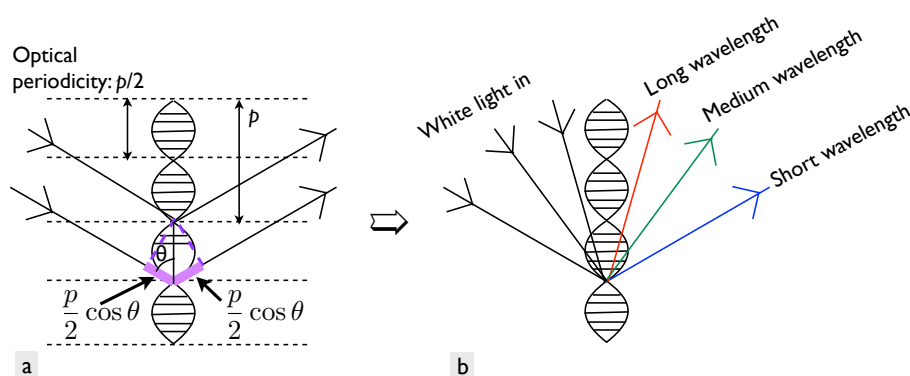


Figure 2: (a) The iridescent colour due to selective reflection from the cholesteric helical structure (exhibiting a photonic band gap due to the period modulation of refractive index) depends on the helix pitch  $p$  but also on the angle of incidence  $\theta$  through the Bragg relation  $\lambda_{air} = p \cos \theta \cdot n_{av}$ , where  $n_{av}$  is the average refractive index of the cholesteric. Inside the cholesteric the constructively interfering, and thus selectively reflected, light has the wavelength  $\lambda_{LC} = p \cos \theta$ . (b) Depending on the angle of incidence  $\theta$  the reflected colour thus changes even for constant cholesteric pitch.

diameter. Smaller droplets can however be readily produced and their optical properties are analogous, as shown in Fig. 3. The fact that they constitute a small fraction of a continuous phase that is liquid however makes it more difficult to bring them into a regular colloidal crystal arrangement, and the smaller scale of the patterns makes the analysis less accurate.

## 2 Corroboration of TIR-mediated photonic cross communication

To confirm that all peripheral spots inside the outermost ring indeed arise from ray paths that include a TIR event at the surface of the continuous phase we conducted an experiment where we added more continuous phase and followed the reflection pattern until equilibrium was reached, cf. Fig. 4 and movie ESI6. The liquid crystal has slightly lower density than the continuous phase, hence the droplets float up to the top of the system, eventually aligning their topmost point with the surface of the continuous phase (the density difference is sufficiently low and the surface tension of the continuous phase sufficiently high that we may neglect the slight modulation of the surface in a first approximation). Directly upon adding more continuous phase the close-packed hexagonal arrangement is disturbed, temporarily bringing the droplets out of the same vertical plane. This means that all peripheral spots disappear briefly, leaving only the fundamental red central spot in each droplet, as seen in Fig. 4a. As the droplets float up towards the raised surface they soon align in a plane again and thus the blue direct reflection ( $D$ ) spots reappear near the perimeter, as shown in panel (b). In this pic-

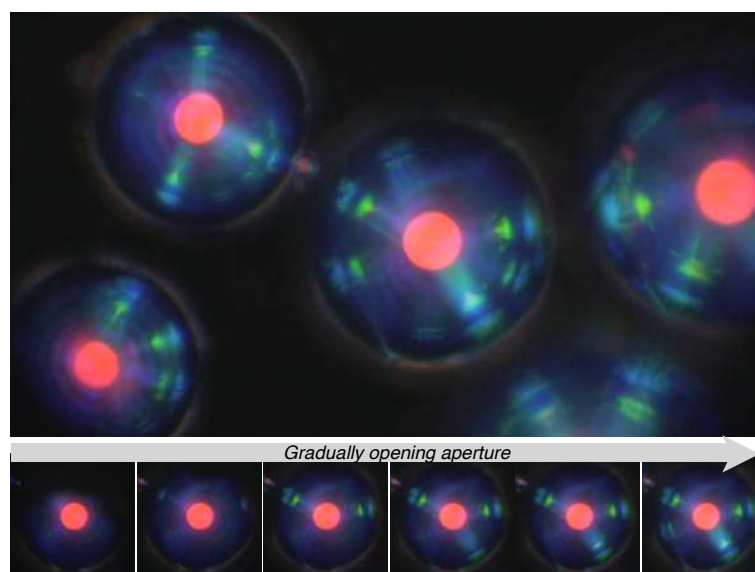


Figure 3: Droplets from a red-reflecting cholesteric mixture of about  $50 \mu\text{m}$  diameter, observed in reflection polarized microscopy. The lower series shows the behavior of the droplet at the center of the upper picture, as the field aperture is gradually opened.

ture sequence the full hexagonal pattern is not visible, indicating that some neighbour droplets have not yet reached the same vertical level as the imaged droplet.

Soon afterwards the droplets have risen sufficiently close to the surface that also the *nn-TIR* spots appear, cf. Fig. 4c. Note that these spots appear with a strong reddish character, reflecting the smaller angle that the relevant incident light ray makes with the droplet radius when the top of the droplet is somewhat below the surface. The smaller angle means that the wavelength is longer, according to the Bragg relation. The droplets continue to move upwards until the top reaches the surface of the continuous phase. In this process the *nn-TIR* spots move further away from the centre, towards the perimeter, and the wavelength is shifted from the red and towards the blue, such that they appear green once steady state has been reached, as shown in panel (d) of the figure. The change in wavelength and position reflects the increase in the reflection angle at the cholesteric droplet interface, as measured from the droplet radius.

### 3 Spectrophotometric analysis of the reflection pattern

In order to corroborate the model with quantitative data we mounted a spectrophotometer (PhotoResearch PR-702A Spectrascan) on the microscope and measured the reflection spectrum from a series of droplets illuminated such that only the main central spot and the peripheral direct communication (*D*) spots appear, cf. Fig. 5. The signal is unfortunately very weak, hence the spectrum is rather noisy, but fitting of two Lorentz functions to the data nevertheless allowed us to establish the reflection wavelengths of

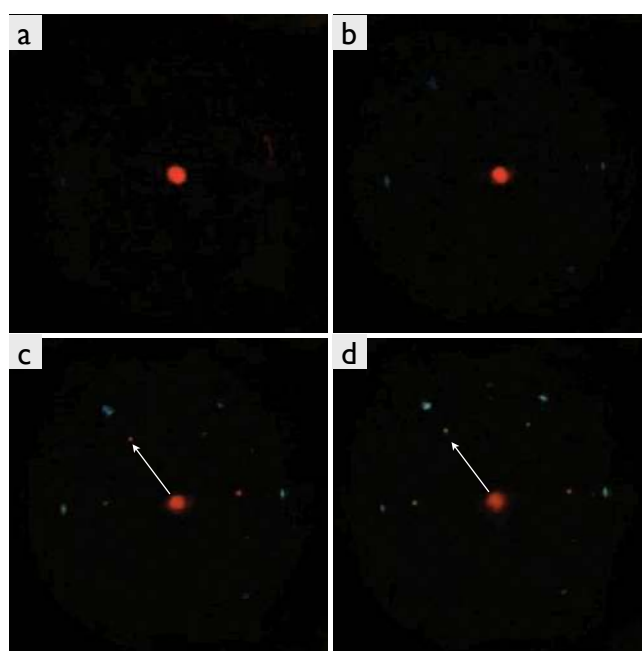


Figure 4: Sequence of inter-droplet photonic communication spots appearing, moving and shifting in wavelength as the surface of the continuous phase is raised (still frames from movie ESI6). In order to make the movement of the *TIR* spots between panels (c) and (d) clearer a white arrow of constant length and inclination has been inserted in these two panels, directed from the central red spot to one of the *nn-TIR* spots.

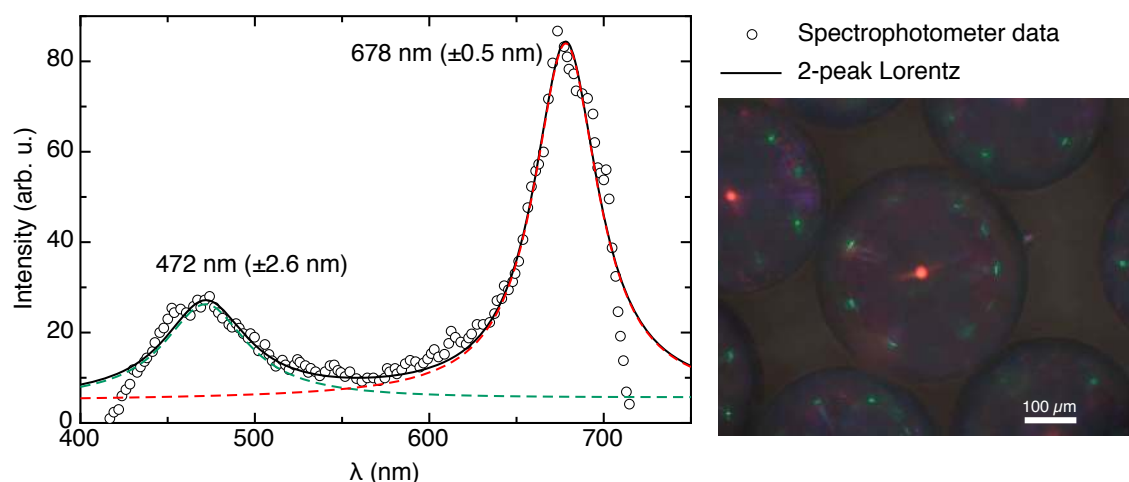


Figure 5: Reflection spectrum from an area with several large droplets of normally red-reflecting cholesteric mixture (shown in the photo).

the two reflections.

For this set of droplets the strongest peak, corresponding to the normal incidence reflection, is located at  $\lambda_0 = 678 \pm 0.5 \text{ nm}$ . The secondary peak, arising from the  $D$  reflections, is centered at  $\lambda_D = 472 \pm 2.6 \text{ nm}$ . For  $\lambda_0 = 678 \text{ nm}$  our basic model predicts that the  $D$  reflections should occur at slightly longer wavelength,  $678 \cdot \cos 45^\circ = 479 \text{ nm}$ . We believe that this discrepancy is due to a slight deformation from perfect spherical shape of the droplets. The liquid crystal has slightly lower density than the continuous phase and buoyancy thus drives them to the sample surface. The surface tension of the continuous phase however pushes the droplets down. Since the droplets are liquid they are deformable, and since the interfacial tension between liquid crystal and continuous phase has been reduced by the PVA stabilizer, the energy cost of deviation from spherical shape is comparatively low. Being squeezed by the oppositely directed forces buoyancy and continuous phase surface tension, the droplets will thus be flattened slightly from perfect sphere to a lightly oblate ellipsoid. This means that the helix axis will be inclined slightly greater than  $45^\circ$  at the point of the droplet where the light meets the surface at  $45^\circ$  angle of incidence, shifting the Bragg reflected wavelength somewhat. Within this model we can establish the actual helix inclination from the fitting results as  $\theta_{eff} = \arccos 472/678 = 45.9^\circ$ , which is a very reasonable value for the lightly oblate droplet.

## 4 Experimental details

*Materials:* The cholesteric ( $N^*$ ) liquid crystal mixtures were composed of the commercial nematic mixture RO-TN 615 from Roche (Switzerland) and the chiral dopant ( $S$ )-4-Cyano-4'-(2-methylbutyl)biphenyl (CB15), purchased from Synthron Chemicals (Germany). The mixtures can be tuned to reflect from the infrared to the ultraviolet

range, with visible normal-incidence reflection occurring for CB15 concentrations between 30 wt.-% and 50 wt.-% (the pitch gets shorter the higher the chiral dopant concentration). For ensuring planar alignment and counteracting coalescence of the liquid crystal droplets, they were dispersed in a continuous phase consisting of a distilled water + glycerol mixture (50/50 volume ratio) in which 3 wt.-% polyvinylalcohol (PVA) was dissolved (Sigma-Aldrich,  $M_w \approx 31,000 - 50,000 \text{ g mol}^{-1}$ , 98-99% hydrolysed).

*Experimental setup:* In order to produce the droplets from cholesteric ( $N^*$ ) liquid crystal mixtures, a nested glass capillary microfluidic setup was built, following the design of Utada et al.[1] The cholesteric liquid crystal mixture is pumped into the PVA solution, flowing coaxially with the liquid crystal, and since the two liquids are immiscible the  $N^*$  stream pinches off into droplets that are highly mono disperse when the correct flow conditions are found. The production was done at room temperature, at which the liquid crystal mixture is in the  $N^*$  phase. This turned out to have a positive effect on the alignment, the resulting circular flow within the droplet most likely favouring a uniform alignment of the director at the edges and thus of the helix. The flow rate of the outer phase was generally 2.7 times higher than that of the liquid crystal. The cholesteric droplets were collected in a flat-based container at high volume fraction until a 2D colloidal crystal arrangement was stabilised. During polarising microscopy investigations a silicon chip was used as substrate in order to avoid unwanted multiple reflections which disturb the image when using a transparent substrate.

## References

- [1] A. Utada, L. Chu, A. Fernandez-Nieves, D. Link, C. Holtze, and D. Weitz, "Dripping, jetting, drops, and wetting: The magic of microfluidics," *Mrs Bull*, vol. 32, no. 9, pp. 702–708, 2007.